

Complex Absorption and Reflection of a Multi-temperature Cyclotron-Bremsstrahlung X-ray Cooling Shock in BY Cam

C. Done¹ and P. Magdziarz^{2,3}

¹*Department of Physics, University of Durham, South Road, Durham, DH1 3LE*

²*Astronomical Observatory, Jagiellonian University, Orla 171, 30-244 Cracow, Poland*

³*N. Copernicus Astronomical Center, Bartycka 18, 00-716, Warsaw, Poland*

15 May 2018

ABSTRACT

We re-analyse the ASCA and GINGA X-ray data from BY Cam, a slightly asynchronous magnetic accreting white dwarf. The spectra are strongly affected by complex absorption, which we model as a continuous (power law) distribution of covering fraction and column of neutral material. This absorption causes a smooth hardening of the spectrum below ~ 3 keV, and is probably produced by material in the preshock column which overlies the X-ray emission region. The ASCA data show that the intrinsic emission from the shock is not consistent with a single temperature plasma. Significant iron L emission co-existing with iron K shell lines from H and He-like iron clearly shows that there is a wide range of temperatures present, as expected from a cooling shock structure. The GINGA data give the best constraints on the maximum temperature emission in the shocked plasma, with $kT_{\max} = 21^{+18}_{-4}$ keV. Cyclotron cooling should also be important, which suppresses the highest temperature bremsstrahlung components, so the X-ray data only give a lower limit on the mass of the white dwarf of $M \geq 0.5M_{\odot}$. Reflection of the multi-temperature bremsstrahlung emission from the white dwarf surface is also significantly detected.

We stress the importance of modelling *all* these effects in order to gain a physically self-consistent picture of the X-ray spectra from polars in general and BY Cam in particular.

Key words: stars: individual: BY Cam – cataclysmic variables – binaries: close – X-rays: accretion – X-rays: accretion

1 INTRODUCTION

Magnetic cataclysmic variables (polars or AM Her stars) are binary systems where a magnetised ($B \sim 10^7$ G) white dwarf accretes from a low mass companion (see e.g. the review by Cropper 1990). Such magnetic fields are strong enough to disrupt disk formation. Instead, the accreting stream is entrained by the magnetic field and falls freely through the gravitational potential until it hits the white dwarf surface. The resultant strong shock has a typical temperature of tens of keV for optically thin material, giving rise to an X-ray emitting plasma. Normally such systems are locked into synchronous rotation by the magnetic field, so that (to zeroth order) the stream impacts onto the same part of the magnetosphere. However, there are now three systems known where the orbital period and white dwarf spin period are slightly different, BY Cam, V1500 Cyg and RXJ 1940.2-

1025 (e.g. Watson et al 1995), so that the accretion geometry changes continuously.

Recent progress in understanding the detailed shape of the X-ray emission has concentrated on the effects of reprocessing of the hard X-ray emission. Inclusion of the effect of Compton reflection from the white dwarf surface *and* complex absorption from the accreting material *and* the multi-temperature shock structure are necessary ingredients in the spectral model. While the importance of any one or two of these individual effects have long been recognised (e.g. Imamura & Durisen 1983 – absorption and shock structure; Swank, Fabian & Ross 1984; Beardmore et al 1995 – absorption and reflection) all three are necessary in order to obtain a self-consistent description of the observed X-ray emission (Done et al 1995; Cropper et al 1997). Both the complex absorption and Compton reflection harden the spectrum,

leading to an overestimate of the plasma temperature. The line emission from the hot plasma gives another independent measure of the plasma temperature, from the ratio of 6.7 and 6.9 keV lines from He- and H-like iron, respectively. The temperature of the line emitting material is then lower than that inferred from the 'observed' continuum. This discrepancy is exacerbated in detectors of low energy resolution as Compton reflection produces a fluorescence iron line at 6.4 keV from the (nearly neutral) X-ray illuminated white dwarf surface, which is then blended by the instrument with the 6.7 and 6.9 keV lines. This reduces the mean iron line energy and leads to an underestimate of the plasma temperature. This systematic mismatch between 'observed' line and continuum temperatures is particularly evident in the large sample of GINGA (low spectral resolution) X-ray spectra of polars (Ishida 1991), even after the inclusion of complex absorption. Both complex absorption *and* Compton reflection are required to obtain consistent temperatures from the line and continuum data (Beardmore et al 1995; Done et al 1995), but then the derived temperature is of order 10 keV, much lower than the expected Rankine-Hugoniot temperature for a strong shock of $\sim 57(M/M_{\odot})(R/5.57 \times 10^8)^{-1}$ keV (e.g. Frank, King & Raine 1992, Imamura et al 1997). Using multi-temperature shock models rather than assuming a single temperature plasma goes some way to resolving this, as the mean temperature of a ~ 30 keV multi-temperature shock structure is ~ 10 keV (Imamura & Durisen 1983; Done et al 1995; Wu, Chanagen & Shaviv 1995; Cropper et al 1997). Cyclotron cooling of the hottest/least dense material probably accounts for any remaining temperature discrepancy (Wu et al., 1995; Woelk & Beuermann 1996).

While much real progress has been made, problems still remain. The most pressing of these have to do with the pre-shock accretion column. This material is irradiated by the X-ray emission, so should have a complex ionization structure (see e.g. Ross & Fabian 1980; Swank et al 1984; Kallman et al 1993, 1996). It is also spatially extended over the X-ray source so that different segments of the X-ray emission travel through different path lengths of the material (Done et al 1995), especially as the accretion column is probably arc-like in cross-section, rather than circular (e.g. Cropper 1990). The column should also add further complexity from secondary emission (Kallman et al 1993, 1996) and scattering (Ishida et al 1997). Models including all these effects are currently being developed (Rainger et al 1997, in preparation), but the situation is clearly complex. Even more degrees of freedom are possible in the models: the material in the column is probably highly inhomogeneous, as dense 'ribbons' of material embedded in a much less dense medium are required in order to explain the soft X-ray excess seen in several of these objects (e.g. Kuijpers & Pringle 1982; Frank, King & Lasota 1988; Ramsay et al., 1994).

BY Cam has been extensively studied by previous X-ray instruments, and its spectrum shows many of the temperature discrepancies discussed above. Kallman et al (1993, 1996) propose an explanation for these in terms of secondary emission from the column, producing an additional source of ionised 6.7 keV iron line emission. Here we reanalyse the GINGA and ASCA data from BY Cam and show that the spectrum is well described by the absorption/reflection/multi-temperature shock picture de-

veloped above, and that the contribution of the pre-shock material to the iron K line emission is probably negligible.

2 OBSERVATIONS

The GINGA data were taken in 1988 February 7–10, with background observations taken directly before and after this. However, the second background could not be used as the ROSAT All Sky Survey Bright Source Catalog gives 3 sources within 35 arcmin of the pointing position with total flux 1/5 of that from BY Cam itself. The first background alone is not sufficiently long to sample all the background conditions seen during the source observation so we exclude those parts of the source data which are not well matched by the background observation. Standard selection and cleaning criteria were then applied to both source and background data, and the data were attitude corrected after a 'local' background subtraction (Hayashida et al 1989; Williams et al 1992), resulting in 46 ks of data.

Ishida et al (1991) describes the time variability of the source during these observations. Clear (though generally partial) eclipses are seen in the first half of the dataset, but are absent in the second half. This is explained as a transition in the accretion geometry from a two pole state, where only one of the accretion regions is periodically eclipsed by the white dwarf surface, to a state where the accretion only takes place onto the non-eclipsing pole (see also Silber et al 1992). We split the data into 3 spectra as in Ishida et al (1991), namely pulse high and pulse low (double pole accretion with the eclipsing pole oriented towards and away from the observer respectively) and flaring (accretion onto a single non-eclipsing pole).

The ASCA data taken on 1994 March 10-11 observations and were previously reported by Kallman et al. (1996). FTOOLS 3.6 was used to generate standard response and arf files. The SIS event files were screened in bright2 mode with 1024-binning. The GIS3 data had to be binned onto 128 channels as the data were taken during the time when the onboard CPU mode was wrongly set. This resulted in a total exposure time of 22000 seconds and total count rate of 3.4 counts per second over the four detectors after the standard reduction. The data were accumulated into one single spectrum as Kallman et al (1996) show no obvious hardness ratio changes. We restricted the energy range to 0.6-10 keV for SIS data and 0.8-10 keV for GIS data, and rebinned to have at least 20 counts per bin as required for validity of the χ^2 statistic. The relative normalization of the detectors was within 10 % from our preliminary analysis, thus we fitted all the spectra as a single data group.

Kallman et al (1996) show the data folded on the polarization period of Mason, Liebert & Schmidt (1989) with arbitrary phase. The orbital coverage is $\sim 85\%$ complete, and shows no evidence for an eclipse. The gaps in phase coverage are in two segments, each of width $\sim 0.07 - 0.08$ in phase. The GINGA eclipse in the pulse state has width ≥ 0.1 in phase (Ishida et al 1991), so it seems unlikely that the ASCA data could have avoided the eclipse altogether. The lack of any convincing ingress/egress in the ASCA data then support (although they cannot confirm) the view that the accretion geometry in BY Cam at the time of the ASCA ob-

servation was analogous to that of the GINGA flaring state data.

3 SPECTRAL FITTING

Version 9.1 of XSPEC (Arnaud 1996) is used to fit the spectra. The `mekal` code is used to model a single temperature hot plasma, while a modified version of the `cevmk1` code (see Done & Osborne 1997) is used for the multi-temperature plasma models which uses Morrison & McCammon (1983) abundance ratios. This gives a spectrum

$$f(\nu) \propto \int_{10^{5.5} K}^{kT_{max}} \frac{\epsilon(n, T, \nu)}{\epsilon(n, T)} \left(\frac{T}{T_{max}} \right)^{\alpha-1} dT$$

where $\epsilon(n, T, \nu)$ is the bremsstrahlung spectral emissivity at a given density n and temperature T while $\epsilon(n, T)$ is the total (frequency integrated) emissivity (see also Done et al 1995). Models with $\alpha = 1$ give a spectrum where each temperature component is weighted by its cooling time, i.e. the spectrum expected from pure bremsstrahlung cooling at constant pressure and gravitational field (see the discussion in Done et al 1995 and references therein).

The reflection code is described in Done et al (1995, 1997), and here we assume a fixed inclination angle to the reflector of 60° . Error ranges are given as $\Delta\chi^2 = 2.7$ unless otherwise stated, although this is an underestimate of the true 90% confidence limits where parameters are correlated.

3.1 ASCA data

Single temperature plasma models, where the abundances of all the elements heavier than He are assumed to scale together, give fairly good fit, with $\chi_\nu^2 = 1458/1272$, but the minimum temperature of $kT = 200_{-35}^{+170}$ keV shows that the continuum is much harder than can plausibly be expected for optically thin accretion onto a white dwarf. Inclusion of an $\alpha = 1$ multi-temperature continuum model does not significantly improve the fit ($\chi_\nu^2 = 1455/1272$), and the derived (maximum) temperature is even higher, with $kT_{max} = 940_{-310}^{+\infty}$ keV, as the multi-temperature spectrum includes the softer cooling components. Clearly there is some distortion present that is hardening the observed spectrum in the ASCA bandpass. Absorption is the most obvious way to do this since Compton reflection only contributes significantly to the spectrum above 5 keV, so is unlikely to strongly affect the ASCA data. Simple absorption (complete covering by neutral material) is already included in the fit, so we try partial covering by neutral material. Ishida (1991) shows that such complex absorption is not uncommon in polars, and uses this model to fit the GINGA data of BY Cam (Ishida et al., 1991). This gives a significantly better fit for the multi-temperature $\alpha = 1$ plasma model, with $\chi_\nu^2 = 1414/1270$ for $N_H = 2.3_{-0.8}^{+1.2} \times 10^{22}$ cm⁻² and $C_f = 0.20 \pm 0.05$ but still results in a physically unreasonable maximum shock temperature of $kT = 165_{-55}^{+100}$ keV. A more realistic shock temperature of $kT = 63_{-15}^{+17}$ keV can be obtained with the single temperature plasma model with $N_H = 2.7_{-1.0}^{+1.8} \times 10^{22}$ cm⁻² and $C_f = 0.15 \pm 0.03$, but at the expense of physical consistency (we expect multi-temperature components to be present) and goodness of fit ($\chi_\nu^2 = 1436/1270$).

The ASCA data extend to substantially lower energies than can be studied with GINGA, and so are more sensitive to the form of the absorber. A partial covering model is an *ad hoc* description of what is expected to be a much more complex situation. A power law distribution of column with covering fraction i.e. $C_f(N_H) \propto N_H^\beta$ (see also Norton, Watson & King 1991) gives a good approximation to the complex absorption expected through neutral material extended over the source (e.g. Done et al 1995). The sum of covering fractions must be unity so that the emergent spectrum $S(E)$ is related to the intrinsic spectrum $S_{int}(E)$ by

$$S(E) = S_{int}(E)A \int_{N_{H,min}}^{N_{H,max}} N_H^\beta \exp(-N_H\sigma(E)) dN_H \quad (1)$$

where

$$A = \frac{\beta + 1}{N_{H,max}^{\beta+1} - N_{H,min}^{\beta+1}} \dots \beta \neq -1$$

$$= \frac{1}{\log(N_{H,max}/N_{H,min})} \dots \beta = -1$$

and $\sigma(E)$ is the photo-electric absorption cross-section from Morrison and McCammon (1983) abundances as given by the `wabs` model in XSPEC. We fix $N_{H,min} = 10^{20}$ cm⁻², and Figure 1 shows the transmitted fraction as a function of energy for $N_{H,max} = 10^{24}$ cm⁻² with β ranging from -1 to 1 . For comparison we also show the transmitted fraction obtained by the circular column model of Done et al (1995) for a mid column of 5×10^{23} cm⁻² (and hence a maximum column of 10^{24} cm⁻²), and that obtained from complete covering by a column of 5×10^{23} cm⁻². The power law absorption model gives a smooth hardening of the spectrum which matches the data significantly better ($\chi_\nu^2 = 1399/1270$) than the partial covering model. The derived maximum temperature of a multi-temperature plasma is then the more physically reasonable $kT_{max} = 45_{-14}^{+35}$ keV for a maximum column of $2.5_{-1.8}^{+\infty} \times 10^{24}$ cm⁻², with index $\beta = -1.07 \pm 0.08$. Figure 2 shows the data and residuals for this model, along with the intrinsic spectrum before the absorption.

Alternatively, the material may be ionized due to the intense irradiation of the pre-shock column by the X-ray emitting plasma. We use the XSPEC model `absori` to approximate this, fixing the power law temperature of the illuminated material to 3×10^4 K and approximating the X-ray spectrum by a power law of photon index $\Gamma = 1.5$. Complete covering by a ionized material gives a worse description of the data, with $\chi_\nu^2 = 1431/1270$ for a column of $5.2_{-2.5}^{+3.5} \times 10^{21}$ cm⁻² at an ionization parameter of $\xi = 240_{-120}^{+160}$, and again with an unphysically high temperature for the $\alpha = 1$ plasma of $kT_{max} = 270_{-100}^{+130}$ keV. Such models have been used above 2 keV to match the complex absorption seen in the data (Beardmore et al 1995; Cropper et al 1997), but they predict a large Oxygen edge which is inconsistent with the observed spectra below 1 keV.

To summarise the results so far, the data strongly require heavy absorption, which significantly hardens the spectrum below 3 keV, but this absorption is complex. Complete covering of the source by a screen of material in a single ionization state (neutral or ionised) is strongly ruled out. Instead the absorption can be described as a continuous range of columns through which the source is seen, as expected for the pre-shock material. While the ionization structure of the

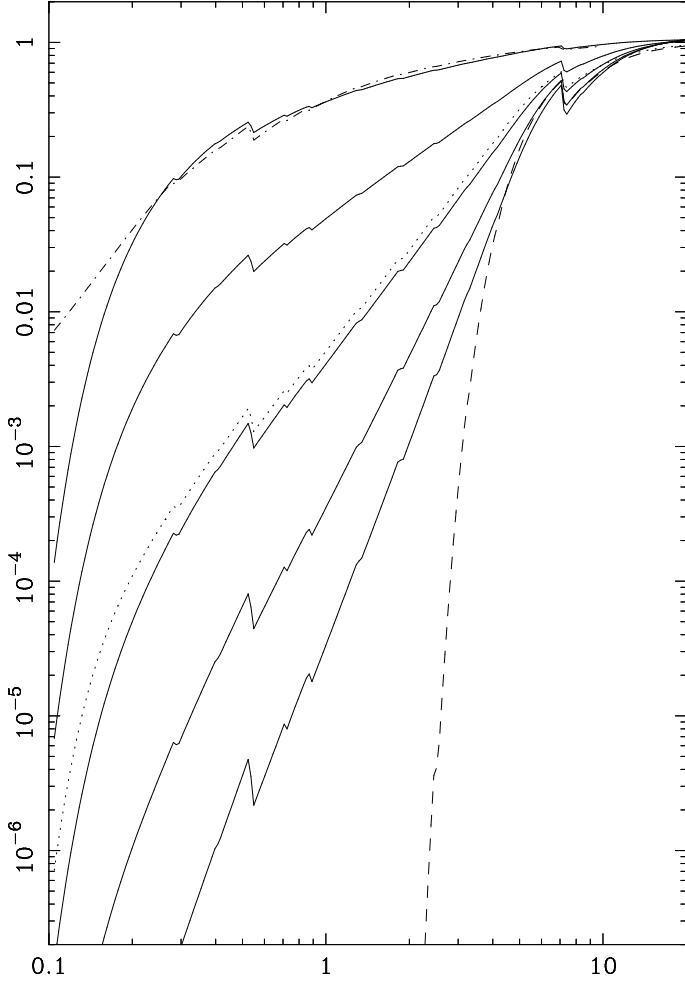


Figure 1. The transmission as a function of energy through neutral material with a power law covering fraction – column distribution for $\beta = -1, -0.5, 0, 0.5$ and 1 from top to bottom. The dotted line shows the transmission through a circular neutral column where $N_{H,mid} = 5 \times 10^{23} \text{ cm}^{-2}$ (Done et al 1995) while the dashed line shows the transmission through a complete screen with $N_H = 5 \times 10^{23} \text{ cm}^{-2}$. The dash-dot line shows the transmission through a circular column with radial density stratification (see Section 4.1).

column is outside of the scope of this paper (see Rainger et al 1997), the data are clearly consistent with a power law column–covering fraction distribution of neutral material, so we use this model in all the following fits. The continuum is also significantly better described by a multi–temperature $\alpha = 1$ cooling shock model than by a single temperature plasma, so we use this to describe the plasma emission in all the following fits.

While the resultant fit is statistically adequate, there are clear residuals left around the iron K line (see Figure 2). Adding a narrow Gaussian line gives a reduction in χ^2_ν to 1363/1268 (significant at greater than 99.9% confidence) for $E = 6.39^{+0.03}_{-0.04} \text{ keV}$ and equivalent width $86^{+36}_{-26} \text{ eV}$. This additional line component is *inconsistent* with being at 6.7 keV, as postulated by Kallman et al. (1996). A (nearly) neutral iron fluorescence line is expected from reflection of the intrinsic spectrum from the white dwarf surface. Fixing the line energy at 6.4 keV and including a neutral Compton re-

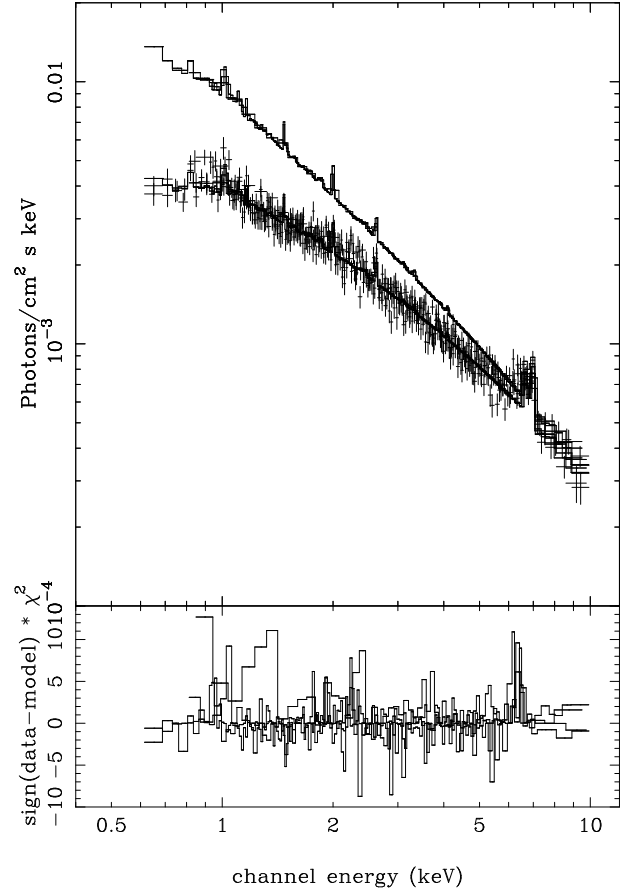


Figure 2. The ASCA spectrum of BY Cam, modelled by a multi–temperature $\alpha = 1$ plasma, absorbed by neutral material with a power law distribution of covering fraction with column. The top panel shows this model and the unfolded spectrum, together with the intrinsic emission before absorption, while the bottom panel shows the remaining residuals to the fit.

flexion continuum that must accompany any reflected line emission leads to $\chi^2_\nu = 1360/1268$, for an amount of reflection $R = 1.5^{+0.6}_{-1.3}$ (where $R = 1$ denotes the normalisation of the reflected continuum expected from an isotropically illuminated slab covering a solid angle of 2π) assuming the abundances in the reflector are the same as those in the hot plasma, with maximum temperature $kT_{max} = 38^{+34}_{-13} \text{ keV}$. While the detection of the reflected continuum is only marginally significant, its level is consistent with that expected from the strength of the cold iron fluorescence line. The line equivalent width and amount of reflection continuum are anti–correlated in the fitting, so a self consistent reflection model (including both line and continuum) would be much better constrained. This fit is detailed in Table 1, and shown in Figure 3.

The abundances of the elements in the hot plasma need not all scale together, especially as BY Cam is proposed to have abundance anomalies to explain the enhanced NV line emission observed in its UV spectrum (Bonnet–Bidaud &

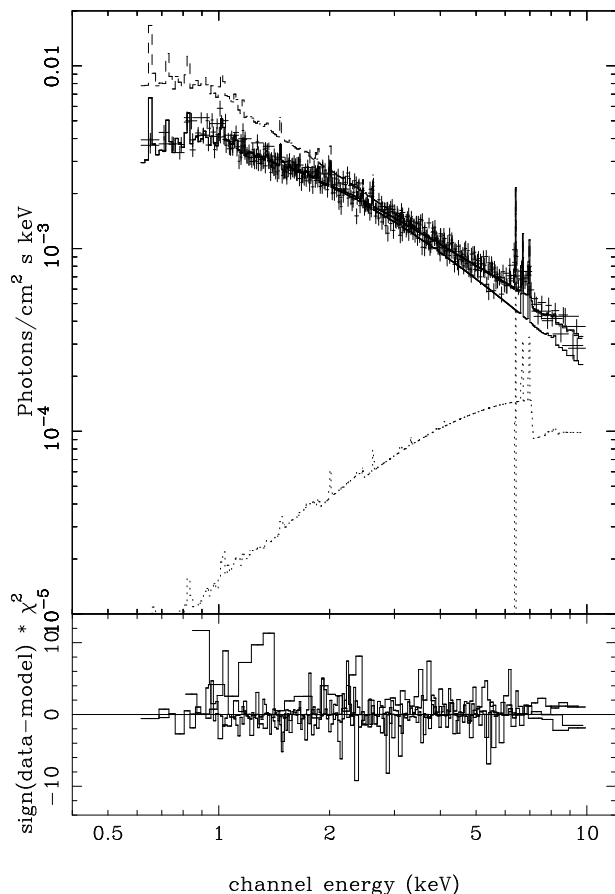


Figure 3. The ASCA spectrum of BY Cam, modelled by a multi-temperature $\alpha = 1$ plasma and its reflection from the white dwarf surface, absorbed by neutral material with a power law distribution of covering fraction with column. The top panel shows this model and the unfolded spectrum, together with the intrinsic emission before absorption, while the bottom panel shows the remaining residuals to the fit.

Mouchet 1987). The N X-ray lines are below the 0.6 keV well calibrated low energy limit of the ASCA detectors, but can be investigated by including the less reliable data down to 0.4 keV. The soft excess is then also apparent (Kallman et al 1996), so a blackbody is needed to model this. The derived limit on the N abundance is then $\leq 15\times$ solar, which is not restrictive. Going back to the standard bandpass, the strongest lines expected at these plasma temperatures are Fe, Si, S and O. Letting the abundances of all these be free gives $A_{Fe} = 0.41^{+0.43}_{-0.12}$, $A_{Si} = 0.69^{+0.30}_{-0.31}$, $A_S = 0.39^{+0.47}_{-0.39}$, $A_O = 0^{+0.29}$ and $A_{rest} = 0.38^{+0.51}_{-0.38}$ with $\chi^2_\nu = 1353/1264$, i.e. there is no significant improvement in the fit as the inclusion of 4 extra free parameters gives a reduction of only $\Delta\chi^2 = 7$. Thus there is no strong evidence for non-solar abundance ratios of the elements, although O is marginally lower than expected.

The intrinsic multi-temperature plasma emission can also be investigated in more detail. We have so far assumed that the plasma cools from the shock temperature to the

white dwarf photosphere at $\sim 10^{5.5}$ K ≈ 27 eV, and that all these cooler components contribute to the spectrum. However, this is not necessarily the case since the cooling plasma may be dense enough to become optically thick, so giving an apparent minimum temperature to the cooling radiation which is rather higher than that of the white dwarf. We modify the plasma emission model to include the minimum temperature as a free parameter of the fit, and find that this converges to an identical fit as before, with $kT_{min} = 27$ eV. The limits on the O abundance are also unchanged, with $A_O = 0^{+0.29}$ ($\chi^2_\nu = 1353/1266$), showing that incomplete cooling is not responsible for any potential deficit of O line emission.

Similarly, the temperature distribution need not be given by the $\alpha = 1$ power law model expected from pure X-ray line and continuum cooling as the assumptions of bremsstrahlung only cooling at constant pressure and gravitational field may not be accurate. Letting α be free gives a significant decrease in χ^2_ν to 1354/1267 for $\alpha = 0.6$ and $kT_{max} = 55$ keV.

Thus the data are consistent with multi-temperature emission from complete cooling behind the shock, where the accreting material is $\sim 0.5\times$ solar abundance in all the elements. This intrinsic spectrum is then modified by reflection from the white dwarf surface, producing both reflected continuum and associated 6.4 keV iron fluorescence line, and further distorted by complex absorption. The intrinsic emission is required to be a multi-temperature plasma, and the cooling components are significantly detected in the data. Parameters for both the expected $\alpha = 1$ cooling model and the better fitting model where α is free are given in Table 1. The best fit single temperature model (including reflection and complex absorption) is also tabulated for comparison, but is a worse fit by $\Delta\chi^2 = 20$ as the data contain significant iron L line emission which cannot be fit by the single temperature models. This is the first observational confirmation of the theoretically expected cooling of the shocked plasma in polars, although the distribution of cool components with temperature is marginally inconsistent with the predicted $\alpha = 1$.

3.2 GINGA data

All 3 GINGA spectra give a lower flux than the ASCA data, even in the overlapping 2–10 keV band. Ratios of these spectra with the best fit ASCA model are given in Figure 4. All the spectra are also systematically different in shape compared to the ASCA data, being generally softer. Thus there are significant spectral as well as intensity changes between the GINGA and ASCA observations.

We first fit the GINGA low and high pulse state data, where the inclination angle to the eclipsing spot is changing with phase. We fit the two datasets simultaneously, constraining the interstellar absorption, plasma temperature and abundances to be the same. Ishida et al (1991) show that complex absorption is required by the data, and model this by partial covering. A single temperature plasma model with partial covering gives $\chi^2 = 37/51$. The low state spectrum is significantly softer than the high state at low energies, and in fact does not require any absorption. Constraining the two partial coverers to be the same gives a much worse fit with $\chi^2 = 56/53$. Replacing the partial coverer by

Table 1. ASCA spectral fitting with multi-temperature (pIT) and single temperature (1T) models

Model	$N_{H,Gal}$	kT ^a (keV)	A ^b	$N^c \times 10^{-2}$	α	R	EW (eV)	$N_{H,max}^d$	β	χ^2_ν
pIT	$0.07^{+0.03}_{-0.04}$	38^{+34}_{-13}	$0.52^{+0.33}_{-0.15}$	7.0	1 ^e	$1.5^{+0.6}_{-1.3}$	75 ± 25	$5.6^{+9.0}_{-2.6}$	$-1.08^{+0.12}_{-0.13}$	1360/1268
pIT	0.09 ± 0.04	55^{+8}_{-22}	$0.45^{+0.30}_{-0.20}$	5.1	0.60 ± 0.25	$1.5^{+0.7}_{-0.6}$	75 ± 25	$4.6^{+7.0}_{-2.6}$	$-1.0^{+0.25}_{-0.15}$	1354/1267
1T	0.06 ± 0.03	18^{+5}_{-6}	$0.49^{+0.20}_{-0.18}$	3.5	∞^e	1.1 ± 0.6	85 ± 25	1000^{+99}_{-997}	-1.23 ± 0.09	1380/1268

^a This is the maximum temperature in the multi-temperature models

^b with respect to Morrison and McCammon (1983)

^c The normalisation of the plasma model in units of $10^{-14}/(4\pi D^2) \times$ Emission Measure

^d Units of 10^{22} cm^{-2}

^e Parameter fixed

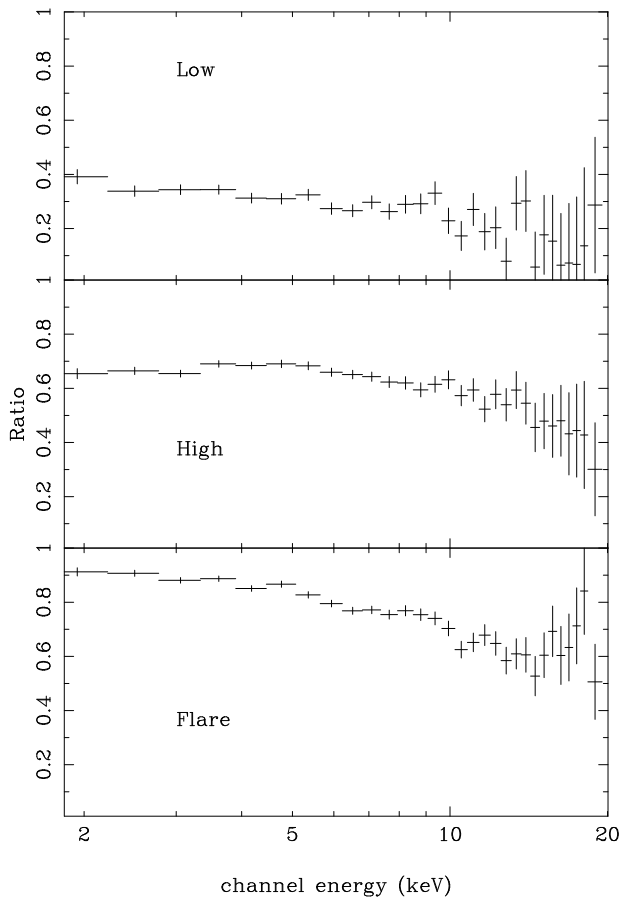


Figure 4. The ratio of the GINGA spectra to the best fit $\alpha = 1$ ASCA spectral model shown in Figure 3. The low pulse phase, high pulse phase and flare spectra are shown in the top, middle and bottom panels, respectively.

the power law column-covering fraction model used for the ASCA data gives an equally good fit, showing that the wider ASCA bandpass is needed to properly constrain the complex absorption properties. We use the power law absorber for consistency with the ASCA results, but since $N_{H,max}$ and β are strongly correlated and poorly determined we constrain β to be equal across all the datasets. This gives $\chi^2_\nu = 35/52$

for $\beta = -1.01 \pm 0.08$, $N_{H,max} = 5.0^{+9.0}_{-4.5}$ and $770^{+99}_{-690} \times 10^{22} \text{ cm}^{-2}$ for the low and high state spectra, respectively.

Again the residuals clearly indicate structure around the iron line and edge energies so we fit a reflection continuum spectrum and 6.4 keV iron fluorescence line. This gives a significant improvement in the fit with $\chi^2_\nu = 28/50$. The continuum was then replaced with the multi-temperature $\alpha = 1$ emission model. This did not give a significantly better fit to the data, showing that the 2–20 keV GINGA bandpass is not sufficient to distinguish between single and multi-temperature emission models. However, we chose this model for further study, for ease of comparison with the ASCA fits. The flaring state spectrum is then also fit with this model, and the results detailed in Table 2. Error ranges on the absorber are not given since this quantity is unconstrained by the data. The harder spectrum seen in the high state can equally well be described by a larger contribution from the reflection continuum as by more absorption.

4 DISCUSSION

4.1 Absorption

The complex absorption is clearly a major component in the spectrum, giving a smooth hardening at energies lower than ~ 4 keV which cannot be described by complete covering by material of a single ionization parameter. The lack of the standard absorption signatures (strong low energy cutoff or ionised edges) means that it is not always obvious that this component is present in the spectrum. In BY Cam its main signature is that the derived temperature for the ASCA spectrum becomes unphysically high without it. We caution that where this complex absorption is present, the observed bremsstrahlung luminosity can be severely underestimated in spectra which only extend to 2–3 keV (e.g. ROSAT; Ramsay et al., 1994).

Our model for this absorption is one in which neutral material with a range of covering fractions obscures the source, so that $C_f(N_H) \propto N_H^\beta$. The simplest geometry of a cylindrical neutral column overlaying a circular source predicts a distribution of column with covering fraction such that $\beta \sim 0$ (see Figure 1). This is very different from the observed $\beta = -1$, indicating that the situation is (unsurprisingly) much more complex.

The absorption can only be constrained by the ASCA data which is phase averaged, so some of the discrepancy in expected column distribution could arise from co-adding

Table 2. Simultaneous spectral fits to the GINGA pulse low (Low), pulse high (High) and flaring data with a multi-temperature plasma continuum, reflection and complex absorption. The temperature of the High and Low pulse states are tied together, while the abundance, temperature distribution and absorption power law are tied across all the datasets.

Data	$N_{H,Gal}$	kT ^a (keV)	A ^b	N ^c × 10 ⁻²	α	R	EW (eV)	N _{H,max} ^d	β	Total χ _ν ²
Low	0.0 ^{+0.52}	21 ⁺¹⁸ ₋₄	0.25 ^{+0.10} _{-0.09}	2.4	1 ^e	1.1 ^{+1.2} _{-1.1}	0 ⁺¹³⁵	1.9 ^{+∞} _{-1.9}	-0.9	41.4/73
High				5.2		1.6 ^{+1.2} _{-1.3}	35 ⁺⁷⁰ ₋₃₅	8.8		
Flaring		25 ⁺¹⁸ ₋₇		6.5		1.0 ^{+1.0} _{-0.9}	45 ⁺⁸⁰ ₋₄₅	4.0		

^a This is the maximum temperature in the multi-temperature models

^b with respect to Morrison and McCammon (1983)

^c The normalisation of the plasma model in units of 10⁻¹⁴/(4πD²) × Emission Measure

^d Units of 10²² cm⁻²

^e Parameter fixed

data. Further distortions could also be produced if the accretion column is ionised. This would have the effect of making the absorption from a circular column less dramatic than predicted from neutral material, as required by the $\beta = -1$ distribution. Photo-ionization of a uniform accretion column has long been known to be likely (Ross & Fabian 1980; Swank, Fabian & Ross 1984) but is much less probable if the column has a highly inhomogeneous 'blobby' structure (e.g. Frank, King & Lasota 1988). In this case radial structure can alter the observed properties. The observed $\beta = -1$ distribution can be reproduced by a model in which neutral blobs accrete preferentially towards the centre of the column, with blob density $\propto r^{-5}$, so that the much less of the X-ray source is covered by the highest column density material (dash-dotted line in Figure 1).

All accretion column models predict a substantial change in absorption with phase. For a neutral, constant density column, there should be much less absorption when the hard X-ray emission region is on the limb of the white dwarf (pulse low state) than when it is viewed more directly (pulse high) as the mean path length through the accretion column is smaller (Done et al 1995). Allowing for ionization enhances this effect, as the high ionization material (and hence weakest absorption) is produced in the layers closest to the shock. The GINGA data are indeed consistent with a change in absorption between low and high state, in the sense that the low state is less absorbed (see Table 2), but a complete model of the density and ionization structure of the photo-ionised column to determine both its absorption and emission properties is clearly needed before such ideas can be properly tested.

The absorption is also presumably linked to the mass accretion rate, as there is more material in the column at high mass accretion rates. Thus for a neutral column we expect that the absorption should correlate with X-ray luminosity. By contrast, an ionised column may show absorption anti-correlated with luminosity as the bremsstrahlung intensity is $\propto n^2$ while the column density is only $\propto n$. Again, proper modelling of the column is required in order to determine the observational consequences of this, and better data are required to test whether the absorber is predominantly ionised or neutral.

4.2 Continuum

A single temperature plasma continuum is clearly ruled out by the ASCA data. Multi-temperature plasma is expected physically, as the hot shocked gas must cool as it emits X-ray radiation. The observational signature of this is that the spectra show significant emission both from the H and He-like K α lines at 6.9 and 6.7 keV and iron L shell lines around 1 keV from much lower ionization species. For all of these different Fe ion states to co-exist requires a multi-temperature plasma. The observed maximum X-ray temperature of 21⁺¹⁸₋₄ keV (from the better constrained GINGA fits) is rather lower than the ~ 57 keV expected from a pure bremsstrahlung shock above a solar mass white dwarf. Taken at face value this would limit the mass of the white dwarf to 0.6^{+0.3}_{-0.1}. However, BY Cam has a substantial magnetic field of ~ 28 MG (Schwope 1996 revised from the Cropper et al 1989 value of 40.8 MG), so cyclotron cooling may be important. The high temperature/low density material close to the shock preferentially cools via cyclotron (emissivity $\propto T^{2.5}n^{0.15}$; Wu et al 1995) while at lower temperatures/higher densities the bremsstrahlung (emissivity $\propto T^{1/2}n^2$) becomes more important. This has the effect of reducing the maximum X-ray bremsstrahlung temperature below that expected from a simple strong shock (Wu et al 1995; Woelk & Beuermann 1996).

Composite cyclotron-bremsstrahlung cooling shocks also have another feature not seen in pure bremsstrahlung shocks, namely that the maximum X-ray temperature *changes* as a function of mass accretion rate. Higher mass accretion rates increase the density of the shocked material, and so shift the balance between cyclotron and bremsstrahlung cooling in favour of bremsstrahlung (Woelk & Beuermann 1996, Wu et al 1995). Thus we expect the maximum shock temperature as seen from the X-ray emission to increase with increasing mass accretion rate. We use the code of Wu et al (1995) to calculate the temperature at which bremsstrahlung and cyclotron cooling are equal for $B = 30$ MG, $M = M_{\odot}$ and mass accretion rate of 3.14 and 6.28×10^{16} g s⁻¹ (corresponding to luminosity of 0.75 and 1.5×10^{34} ergs s⁻¹, respectively). This gives $T_{\max} \sim 25$ and 35 keV. These are intriguingly close to the best fit derived maximum temperatures for the $\alpha = 1$ GINGA and ASCA data of 20 and 38 keV, respectively, for a factor of ~ 2 difference in mean 2–10 keV count rate. While the large error bars mean that the effect is not significant here, these tempera-

ture changes should be seen in high quality, broad bandpass spectra from SAX and/or XTE

Cyclotron cooling has a strong and variable effect in suppressing the high temperature X-ray emission. These BY Cam data stress again the point made by Wu et al (1995) and Woelk & Beuermann (1996) that equating the maximum bremsstrahlung temperature to the shock temperature is *not* a good guide to the white dwarf mass. However, downstream from the shock, once the density and temperature are such that bremsstrahlung dominates the cooling then the shock structure is again given by the standard bremsstrahlung $\alpha = 1$ cooling. This can be seen from the results of the code of Wu et al (1995) and also theoretically, since when bremsstrahlung cooling dominates all the equations are the same as for a bremsstrahlung only shock. The derived temperature distribution seen in the ASCA data is (marginally) significantly different from this, with $\alpha \sim 0.6$ i.e. more cool components than expected. This may be an artifact of the *ad hoc* absorption model used (see above). If the real absorber includes complex contributions from ionised material then some structure should be present at the OVIII K and Fe L line and edge energies which may distort the derived continuum. Alternatively, this may be a real effect, showing that the shock structure deviates significantly from that expected, perhaps due to conduction and/or Compton cooling (Imamura & Durisen 1983; Imamura et al 1987).

4.3 Abundances

The X-ray line emission from BY Cam is weaker than expected from solar abundance (Morrison and McCammon 1983) coronal models. This has been seen systematically from many classes of objects, including stellar coronae (see e.g. Guedel et al 1997; Mewe et al 1997) as well as other Cataclysmic Variables (Done et al 1995; Done & Osborne 1997). While deviations from coronal equilibrium may be expected, none of these seem able to produce the observed weak lines (Done et al 1995, Done and Osborne 1997), so it seems more likely that this represents a true under-abundance with respect to solar. This seems more plausible now that optical studies suggest stars in the solar neighbourhood have considerable dispersion in metallicity, and that the mean $[\text{Fe}/\text{H}]$ is 0.25-0.3 dex *lower* than that of the Sun (Edvardsson et al 1993), but is still an uncomfortable conclusion.

Strong UV lines from NV have led to a claim that the N abundance is enhanced (Bonnet-Bidaud & Mouchet 1987). X-ray line strengths from H and He-like ions give much less ambiguous determinations of abundances than UV or optical photo-ionised lines, but the X-ray N lines are below the well calibrated energy limit of the detector and the derived limit of $\leq 15\times$ solar is not restrictive. Whether or not N is indeed enhanced, the suggested explanation of a recent novae explosion as the cause (Bonnet-Bidaud & Mouchet 1987) seems unlikely since the lines arise from the accretion stream i.e. material from the *secondary* star. Even if the secondary did manage to capture some fraction of the nuclear processed material, the elemental abundance anomalies would become diluted by mixing with the un-reprocessed material in the stellar atmosphere. However, recent HST spectra of the surface layers of the accreting white dwarf in VW Hydri also seem to show abundance anomalies, with Al $\sim 15\times$ solar, and P $\sim 900\times$ solar (Sion et al 1997)! Again, these have

been interpreted as being indicative of a recent novae, so we examine other possible X-ray signatures of nuclear reprocessing in BY Cam.

The core composition of the accreting white dwarf can either be CO or ONeMg. For a CO white dwarf, calculations by Kovetz & Prialnik (1997) show that while N is almost always enhanced in a nova explosion, the O abundance can be almost unaffected or strongly depleted, while the heavier elements are not substantially enriched. This is consistent with the ASCA observations. Conversely, for an ONeMg white dwarf core, $\text{N}/\text{O} \leq 1$ requires that the abundances of P and S should also be strongly enhanced (Politano et al 1995). This type of nova explosion can then be clearly ruled out since S is not overabundant (see Section 3.1). Thus if a recent novae has enriched the N abundance, it would have to be from accretion onto a CO core, although a more likely explanation for anomalous C/N ratios is that the secondary is evolved (Mouchet et al 1997).

4.4 Comparison with previous work

Physically motivated (as opposed to phenomenological) descriptions of the spectrum of BY Cam are given by Kallman et al (1996), using the same ASCA data as studied here. However, their conclusions are rather different in that they propose a strong *line emission* component at 6.7 keV from the pre-shock column, rather than absorption. They require this because their assumed continuum form (a 30 keV bremsstrahlung) produces copious 6.9 keV line from H-like iron, but has a low He-like iron ion fraction, so cannot produce much of the observed 6.7 keV line. We show that this conclusion is obviated by using a continuum given by the (physically expected) multi-temperature plasma emission from a cooling shock, as this can produce both the 6.7 and 6.9 keV lines. Kallman et al (1996) discount this possibility due to the weakness of the observed 6.9 keV line compared to that expected from lower temperature plasma with solar abundances. This objection is removed by allowing iron (and the other element abundances) to be sub-solar. Kallman et al (1996) also comment that with lower temperature plasma the observed continuum is too flat. In our analysis this is resolved by the inclusion of complex absorption from the column. We note that Kallman et al (1996) require a pre-shock column of order $\sim 10^{23} \text{ cm}^{-2}$ overlaying the X-ray emission region. Thus their model is not self-consistent as it does not take into account the strong absorption that this predicts. Our model is also inconsistent in not including the *emission* from the X-ray illuminated column, but the sub-solar iron abundances means that any predicted iron K line emission is reduced by a factor 3 below that of Kallman et al (1996) i.e. ≤ 25 eV equivalent width, which is smaller than the error bars. The photo-ionised column is instead expected to produce the bulk of its emission from continuum/recombination continuum/lines at energies below ~ 1 keV, as noted by Kallman et al (1993) where a large neutral absorption column is required to suppress the strong predicted low energy emission.

Kallman et al (1996) also speculate on the presence of a reflection component to produce the observed 6.4 keV line. Their derived limit of $\Omega/2\pi \leq 0.6$ is again assuming solar abundances, without including the inclination effects, and using the results of early reflection calculations, which gave

EW $\sim 210\Omega/2\pi$ eV for a 20 keV bremsstrahlung illumination. More recent Monte–Carlo results (e.g. George & Fabian 1991, Matt, Perola & Piro 1991, Van Teesling, Kaastra & Heise 1996), scaled to a 20 keV bremsstrahlung continuum (e.g. Beardmore et al 1995) indicate that even for a face on, solar abundance slab the line emission is no more than $\sim 150\Omega/2\pi$ eV, while for a mean (phase averaged) viewing angle of 60° this reduces to $\sim 110\Omega/2\pi$ eV, while abundances of $\sim 0.4\times$ solar reduces it further to $\sim 90\Omega/2\pi$ eV (George & Fabian 1991). Thus the 6.4 keV line strength is easily consistent with reflection from a shock just above the white dwarf surface i.e. with $\Omega/2\pi \sim 1$.

5 CONCLUSIONS

The BY Cam data from ASCA and GINGA give a physically self consistent picture of an accretion column shock, cooling by both cyclotron and bremsstrahlung emission. This multi-temperature X-ray continuum illuminates the white dwarf surface, producing a reflection continuum and iron fluorescence line. Absorption from the pre-shock column strongly modifies the observed spectral form, and is a significant source of uncertainty since it depends on whether the pre-shock column is uniform, or blobby (and hence ionised or nearly neutral), circular or arc-like in cross-section and whether there is radial density structure. We model this absorption by neutral material where the covering fraction is a power law function of the column. This could represent a physical situation where the column is blobby (unionised), with more blobs accreting towards the centre of a circular column. However, it is more likely that this form merely gives a suitable approximation to a more complex situation, and we urge further theoretical modelling of the pre-shock flow.

The multi-temperature emission and reflection model, together with the power law neutral absorption model will be made publically available in the next release of XSPEC.

6 ACKNOWLEDGMENTS

We thank Dave Smith for his help with the GINGA data extraction, and Mark Cropper for useful conversations and the use of his bremsstrahlung–cyclotron cooling code. CD acknowledges support from a PPARC Advanced Fellowship, and PM acknowledges support from Polish Academy of Sciences and The Royal Society. This research has been supported in part by the Polish KBN grant 2P03D01008 and has made use of data obtained through the High Energy Astrophysics Science Archive research Center Online Service, provided by the NASA/Goddard Space Flight Center, and from the Leicester Database and Archive Service at the Department of Physics and Astronomy, Leicester University, UK.

REFERENCES

Arnaud K.A., 1996, *Astronomical Data Analysis Software and Systems V*, eds. Jacoby G. and Barnes J., p17, ASP Conf. Series volume 101

- Beardmore A P, Done C, Osborne J P & Ishida M 1995, *MNRAS*, 276, 483
- Bonnet–Bidaud J.M., Mouchet M., 1987, *A&A*, 188, 89
- Cropper M., Ramsey G., Wu K., 1997, *MNRAS*, in press
- Cropper M., 1990, *Sp. Sci. Rev.*, 54, 195
- Cropper M., et al., 1989, *MNRAS*, 236, 29P.
- Done C., Osborne J.P., 1997, *MNRAS*, in press.
- Done C., Osborne J.P., Beardmore A.P., 1995, *MNRAS*, 276, 483
- Done C., Mulchaey J.S., Mushotzky R.F., Arnaud K.A., 1992, *ApJ.*, 395, 275
- Edvardsson B., Andersen J., Gustafsson B., Lambert D.L., Nissen P.E., Tomkin J., 1993, *A&A*, 275, 101.
- Frank J., King A.R. & Raine D., 1992, In “Accretion power in Astrophysics”, 2d edition, Cambridge, UK: Cambridge University Press
- Frank J., King A.R. Lasota J.–P., 1988, *A&A* 193, 113
- George I. Fabian A.C., 1991, *MNRAS*, 249, 352
- Guedel M., Guinan E.P., Mewe R., Kaastra J.S., Skinner S.L., 1997, *A&A*, 479, 416
- Hayashida K., et al., 1989, *PASJ*, 41, 373
- Imamura J N, & Durisen R H 1983 *ApJ*, 268, 291
- Imamura J.N., Durisen R.H., Lamb D.Q., & Weast G.J., 1987, *ApJ.*, 313, 298.
- Ishida M., 1991, PhD thesis, U of Tokyo
- Ishida M., Silber A., Bradt H.V., Remillard R.A., Makashima K., Ohashi T., 1991, *ApJ.*, 367, 270
- Ishida M., Matsuzaki K., Fujimoto R., Mukai K., Osborne J.P., 1997, *MNRAS*, 287, 651.
- Kallman T.R., Mukai K., Schlegel E.M., Paerels F.B., 1996, *ApJ.*, 466, 973
- Kallman T.R., et al., 1993, *ApJ.*, 411, 869.
- Kuijpers J., Pringle J.E., 1982, *A&A.*, 114, L4
- Kovetz A., Prialnik D., 1997, *ApJ.*, 477, 356
- Mason P.A., Liebert J., Schmidt G.D., 1989, *ApJ.*, 346, 941.
- Matt G., Perola G.C., Piro L., 1991, *A&A*, 247, 25
- Mewe R., Kaastra J.S., Van den Oord G.H.J., Vink J., Tawara Y., 1997, *A&A*, 320, 147.
- Morrison R., McCammon D., 1983, *ApJ*, 270, 119
- Mouchet M., Bonnet–Bidaud J.M., Somov N.N., Somova T.A., 1997, *A&A.*, in press.
- Norton A.J., Watson M.G., King A.R., 1991, *Lecture Notes in Physics Vol 385*, eds Treves A., Perola G.C., Stella L., Springer–Verlag, p155
- Politano M., Starrfield S., Truran J.W., Weiss A., Sparks W.M., 1995, *ApJ.*, 448, 807.
- Rainger J.F., et al 1997, in preparation.
- Ramsay G., Mason K.O., Cropper M., Watson M.G., Clayton K.L., 1994, *MNRAS*, 270, 692
- Ross R., Fabian A.C., 1980, *MNRAS*, 193, 1P
- Schwope A.D., 1996, *Cataclysmic Variables and Related Objects*, p189 Kluwer, Dordrecht.
- Silber A., Bradt H.V., Ishida M., Ohashi T., Remillard R.A., 1992, *ApJ.*, 389, 704
- Sion E.M., Cheng F.H., Sparks W.M., Szkody P., Huang M., Hubeny I., 1997, *ApJ. Lett.*, 480, 17
- Swank J.H., Fabian A.C., Ross R., 1984, *ApJ.*, 280, 734.
- Van Teeseling A., Kaastra J.S., Heise J., 1996, *A&A*, 312, 186
- Watson M.G., et al., 1995, *MNRAS*, 273, 681
- Williams O.R., et al., 1992, *ApJ.*, 389, 157
- Woelk U., Beuermann K., 1996 *A&A*, 306, 232
- Wu K., Channugam G., Shaviv G., 1995, *ApJ.*, 455, 260.